Effects of Compressed Sensing Reconstruction on Kurtosis Tensor Fitting in Diffusion Spectrum Imaging

Jonathan I. Sperl[1], Marion I. Menzel[1], Ek T. Tan[2], Kedar Khare[2], Kevin F. King[3], Christopher J. Hardy[2], and Luca Marinelli[2]
[1]GE Global Research, Garching n. Munich, BY, Germany, [2]GE Global Research, Niskayuna, NY, United States, [3]GE Healthcare, Waukesha, WI, United States

Introduction

Diffusion tensor imaging (DTI) is used clinically to derive angular information of diffusivity in the brain. Diffusion spectrum imaging (DSI) [1], in which the diffusion encoding space (*q-space*) is Nyquist sampled, can be seen as an extension of DTI because it also provides radial information, such as diffusional kurtosis. Kurtosis characterizes the deviation from regular Gaussian diffusion and is expected to be a bio-marker for traumatic brain injury [2] and multiple sclerosis [3].
Clinical investigation of kurtosis requires a fast kurtosis fitting technique such as linear least-squares methods [4]. However, due to the non-Gaussian noise distribution in DSI, these approaches will induce a bias on the fitted tensor elements and the subsequently derived scalar measures such as mean kurtosis or Kelvin eigenvalues [5]. While compressed sensing (CS) may be applied to shorten the long acquisition time of DSI [6], its reconstruction step also has denoising properties, which will influence the accuracy of kurtosis metrics. This work analyzes the effects of CS undersampling and reconstruction on kurtosis estimation.

Theory

As illustrated in Fig. 1, the initial step of a CS-DSI experiment is the generation of a random undersampling pattern on a Cartesian q-space grid. The pattern is converted to a set of diffusion-encoding gradients (with directions n_m and strengths b_m) and data are acquired using these encodings. The undersampled data are fed into a CS reconstruction, which completes the q-space data needed to fit diffusion and kurtosis tensors. Finally, scalar metrics are derived from both tensors.
Given the undersampled q-space signal y, the CS reconstruction is done by computing the data x in the reciprocal *r-space* by solving

$$\min_x \|Ax - y\|_2 + \lambda\|\Psi x\|_1$$

with $A=MF$ (undersampling operator and Fourier transform) and Ψ a sparsifying transform (total variation or wavelets) using a standard iterative shrinkage algorithm [7]. Its solution in r-space is then Fourier transformed back to q-space yielding a fully sampled data set. Optionally, the measured samples may be finally used to replace the reconstructed values via data feedback (DFB).
Fitting is done using a constrained linear least squares method. The kurtosis expansion of the Gaussian diffusion reads

$$\hat{S}(b,n) = S_0 \exp\left(-b\sum_{i,j} n_i n_j D_{ij} + \frac{1}{6}b^2 \mathrm{MD}^2 \sum_{i,j,k,l} n_i n_j n_k n_l W_{ijkl}\right)$$

with S_0 the signal for $b = 0$, D_{ij} the elements of the diffusion tensor, MD the mean diffusivity, and W_{ijkl} the elements of the kurtosis tensor. Fitting the logarithm of the model to the logarithm of the data $S(b_m,n_m)$ is a linear least squares problem. It can be solved analytically using the pseudo-inverse of the system matrix or – if linear constraints are included, e.g. to ensure positive definiteness of the tensors – via quadratic programming [4].
MRI signals are complex valued and the standard assumption for the incorporated noise is white Gaussian noise on real and imaginary parts. CS-DSI processing is based on signal magnitudes and therefore the data are corrupted with Rician noise. Fitting these raw data directly yields biased results, in particular an overestimation of kurtosis [8]. On the other hand, one of the features of CS reconstruction is nonlinear denoising. In the context of DSI this means that CS reconstructions are assumed to be less affected by noise, yielding an improved estimation of the fitted tensors, in particular a reduced bias in the kurtosis.

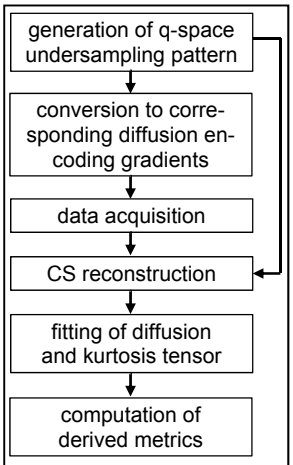

Fig. 1: CS-DSI Workflow

Methods

Fiber simulations were performed using a Gaussian Mixture Model (2 fibers, fractional anisotropy FA=0.85, enclosed angle 30°) on a 17^3 q-space cube. 100 different instances of complex Gaussian noise with different noise levels were added. The q-space data were randomly undersampled with acceleration factor R=4 using 5 different patterns. Total variation-based CS reconstruction was performed. Diffusion and kurtosis tensors were fitted for fully sampled data, undersampled data, and CS reconstructed data (with and without DFB) and the errors of the estimated kurtosis were evaluated.
DSI experiments on healthy volunteers were performed using a 3T GE MR750 clinical MR scanner (GE Healthcare, Milwaukee, WI, USA), equipped with an 8 Channel Head Coil (*TE =141 ms, TR = 3 s, 128x128, FOV = 25 cm, slice = 4 mm, b_{max} = 6,000 s/mm^2*), with data acquired on a 11^3 q-space cube. Tensor fitting was done for the fully sampled data as well as for artificially undersampled (acceleration R=4) and CS reconstructed data without DFB.

Results and Discussion

Fig. 2 shows means and standard deviations of two exemplary kurtosis measures (minimum apparent kurtosis coefficient (AKC), i.e. kurtosis in the direction of one of the two angle bisectors of the two fibers), and mean kurtosis at different noise levels. The bias is clearly reduced for the CS reconstructed data as compared to fully sampled data. DFB should not be used.
Fig. 3 shows kurtosis for brain data. CS reconstruction yields significantly reduced kurtosis. Although no ground truth is available for in-vivo measurements, the simulation results suggest these values to reflect kurtosis in the brain more realistically. Hence the use of CS reconstruction not only helps to accelerate DSI, its denoising properties may also reduce errors in derived metrics like kurtosis, thereby enabling linear least squares fitting to be a fast and robust alternative to more complicated techniques like maximum-likelihood approaches [8].

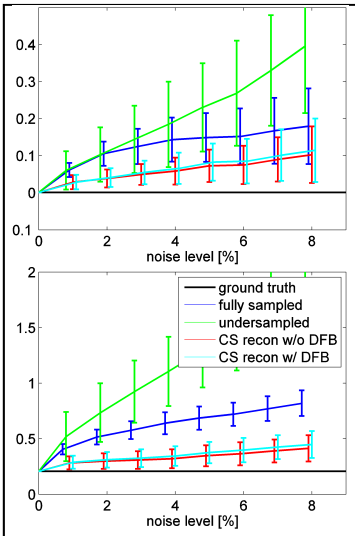

Fig. 2: Fiber simulation results: mean over all noise instances and patterns ± standard deviation of minimum AKC (top) and mean kurtosis (bottom).

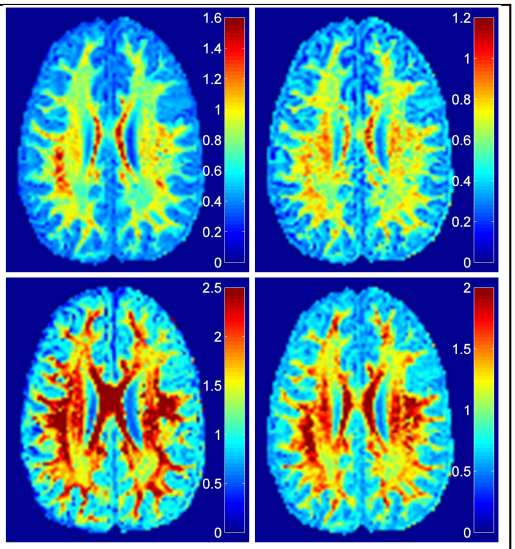
Fig. 3: Mean kurtosis (top row) and maximum Kelvin-Eigenvalues (bottom row) for fully sampled (left) and CS-reconstructed (right) data. Note the different color maps.

References

[1] Wedeen *et al.*, MRM 2005
[2] Inglese *et al.*, NMR Biomed. 2010
[3] Rovaris *et al.*, Neurology 2005
[4] Sperl *et al.*, ISMRM 2011
[5] Qi *et al.*, J. Math. Anal. Appl. 2009
[6] Menzel *et al.*, MRM 2011
[7] Daubechies *et al.*, Commun. Pure Appl. Math 2004
[8] Veraart *et al.*, MRM 2011